American Mineralogist, Volume 70, pages 794–804, 1985

A spectroscopic study of irradiation coloring of amazonite: structurally hydrous, Pb-bearing feldspar

ANNE M. HOFMEISTER[1] AND GEORGE R. ROSSMAN

Division of Geological and Planetary Sciences[2]
California Institute of Technology, Pasadena, California 91125

Abstract

Irradiation-induced color in amazonite can develop only in potassium feldspar having both structurally bound H_2O and Pb impurities. Amazonite color is controlled by either (1) an absorption minimum in the β spectrum between three overlapping bands in the ultraviolet and a broad band at 625 to 643 nm, resulting in a blue color, (2) a combination in β of one UV band and a broad band at 720 nm, resulting in a green color, or (3) both of the above superimposed, resulting in a blue-green color. All optical variations correlated with an EPR pattern indicative of Pb^{3+} or Pb^{1+}. The different types of color are associated with a limited range in Pb content and structural state. For constant Pb content, the intensity of color is linearly related to the amount of structurally bound H_2O, up to a limiting value. Dependence of color intensity on both Pb and H_2O concentration strongly suggests that lead and water occur in a 1 :1 ratio in the color centers. The first order reaction kinetics of amazonite color formation by irradiation and the observation that water is not consumed in the process suggests that water plays a catalytic role in the irradiative transformation of Pb^{2+} to the amazonite chromophore.

Introduction

The color of the blue-green varieties of microcline and orthoclase (amazonite) is radiation-induced (Przibram, 1956, p. 253). Chemical data indicate lead to be the coloring agent (Foord and Martin, 1979), yet Pb^{2+} cannot be the sole cause of the color because all electronic transitions of Pb^{2+} occur in the ultraviolet region. E. E. Foord (pers. comm.) has shown that amazonites with less than 1000 ppm Pb are blue, whereas those with a higher lead content are green, and that the apparent intensity usually increases with lead enrichment. However, some feldspars with as much as 1000 ppm Pb are not colored (Foord and Martin, 1979). Using electron paramagnetic resonance (EPR) techniques, Marfunin and Bershov (1970) concluded that Pb^{1+} centers are present in amazonites, but not in other feldspars. Tarashchan et al. (1973) found that the intensity of an ultraviolet absorption band in amazonite, attributable to a Pb^{2+} transition, increased upon heating but decreased upon subsequent irradiation, and suggested that radiation converts Pb^{2+} to Pb^{1+}. However, Spelt and Lehmann (1982) did not find the Pb^{1+} EPR signal in Australian amazonite. Equally mysterious is the correlation between loss of color and weight loss during dehydration of amazonite (Plyusnin, 1969) because neither H_2O nor OH^- alone can produce color.

The present paper presents and correlates EPR spectra with optical absorption spectra of amazonites and other potassium feldspars in an attempt to establish the origin of color and its relationship to water in the feldspars.

Experimental

Optical absorption spectra were obtained from optically oriented polished slabs of feldspar using calcite polarizers in a Cary 17I spectrometer. Infrared spectra were obtained with gold wire grid polarizers in a Perkin Elmer 180 spectrometer. Both visible and IR spectra were digitized and scaled, but only the visible data required a baseline subtraction. Data from computer peak-fitting did not give accurate areas for the peaks because the baseline (which is a combination of a UV tail and scattering) could not be adequately modelled. Therefore, the baseline was drawn in by hand, and the integrated intensity was estimated by multiplying the peak height by the full width at half height ($W_{1/2}$). Because this approach precludes resolution of two overlapping components, average intensity and total areas are reported for doublets.

EPR spectra were taken at 78 K on a Varian E-line spectrometer at about 9.2 GHz. All samples were coarsely-ground powders weighing about 100 mg. Doubly integrated intensities were calculated from the empirical formula

$$\mathrm{DII} = \frac{(\text{signal height})\cdot(\text{signal width})^2}{(\text{gain})\cdot(\text{sample weight})\cdot(\text{modulation amplitude})\cdot(\text{power})^{1/2}} \quad (1)$$

(Eaton and Eaton, 1979). Also, a line integral was applied twice to doubly integrate digitized and baseline-subtracted first derivative spectra. Because the numerically calculated value depends linearly on the formula-calculated value, and the numerical method is less

[1] Present Address: Geophysical Laboratory, Carnegie Institution of Washington, Washington, D.C. 20008.

[2] Contribution Number 4050.

0003–004X/85/0708–0794$02.00

precise due to baseline approximation, the data from equation (1) are given.

Samples were irradiated at room temperature in air with a ^{137}Cs source which produces 0.66 MeV gamma rays in doses of 1.41 MRads/day. Dehydrations were done in air at 200 to 1000°C.

Water contents of selected samples were measured with a hydrogen extraction apparatus (e.g. Friedman, 1953). The measurements are precise (approximately ±1%), but the amount of water evolved may involve a blank of 1 μmole H_2O (R. E. Criss, pers. comm., 1982) which increases the uncertainty to about ±5%. Three crystals were measured several times to determine the reproducibility. Samples 5 and 25 gave consistent results, but the water content varied by a factor of two for sample #12 which was inhomogeneously turbid from fluid inclusions. Water contents of all other feldspars were determined by comparison of their infrared spectra to that of a feldspar with measured H_2O content and similar spectral features.

Most of the feldspars were provided by E. E. Foord and are described by Foord and Martin (1979) and Foord et al. (in prep.). The feldspars embrace the known range of color and lead content (Table 1), and include the exceptions (#14, 15, 18, 22, 9, 20, 26) to trends of hand-specimen color with chemistry (E. E. Foord, pers. commun.).

Visible spectroscopy of amazonite

General properties

Greenish-blue amazonites are the most common, but the apparent color encompasses values between this and green with a slight amount of yellow (Table 1). Occasionally superimposed on the green is a grey cast due to various oxygen-cation hole centers (Hofmeister and Rossman, 1985).

Absorption spectra of all amazonites examined have the following features in common: (1) The color is intrinsic. (2) All bands are strongly polarized in the beta direction (perpendicular to (001)), and weakly polarized in alpha, perpendicular to (010). Very weak components in the gamma direction were ignored because these are due to scattering, being highest for the most turbid microclines and zero for the nearly gem quality orthoclases. (3) The spectra are dominated by a single band or two overlapping broad bands with total width $W_{1/2}$ of 3000 to 4500 cm-1 which are slighly asymmetric and centered at 625 to 720 cm. (4) The combination of near-IR bands with UV absorption produces a transmission minimum in the blue-green region, giving amazonite its range of colors.

There are four distinct color types (Table 2): (1) type B, common blue, low Pb microcline-perthites possessing three broad polarized absorptions at 625, 385, and 330 nm along with a UV tail (Fig. 1a); (2) type G, end-member green, high Pb orthoclase with $\Delta_{131,1\bar{3}1} \sim 0$ (Cech et al., 1971) consisting of one band at 720 nm plus a UV tail (Fig. 1b); (3) type D: superposition of these two end-member spectral types gives a doublet (Fig. 1c) in intermediate Pb-content microclines; the variation in relative intensity of the 720 and 630 nm peaks produces a gradual shift in the transmission minimum, resulting in the continuous variation of hue from blue-green to green; (4) type T, a turquoise color is produced by a peak at 643 nm (Fig. 1d) which is slightly broader than the 630 nm peak but is not resolvable into a

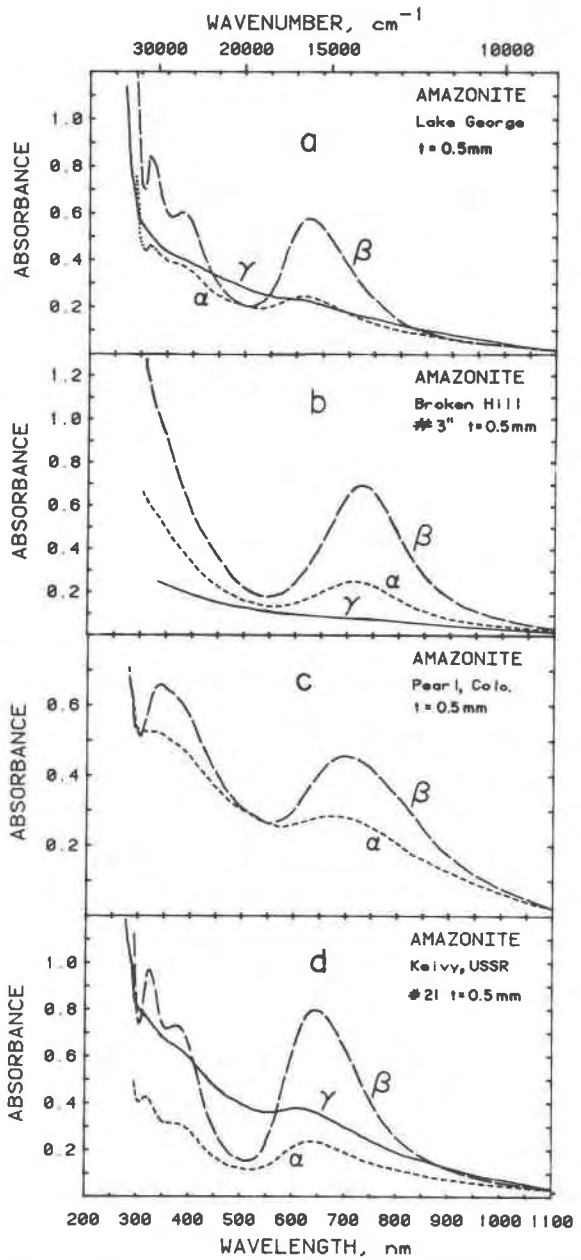

Fig. 1. Polarized absorption spectra of natural amazonites at 23°C. (a) Blue, type B amazonite #5 from Lake George, Colorado. The finely spaced dots indicate where the alpha spectrum was estimated from a spectrum of the same chip after irradiation. The slow rise toward the UV is due to scattering from turbid regions, and from the perthite lamellae. (b) Green, type G amazonite #3" from Broken Hill, Australia. This sample is close to gem quality so that very little scattering contributes to the spectra. The weak band near 360 nm was induced by baseline corrections. The UV tail is markedly polarized in the same scheme as the amazonite peak at 720 nm. (c) Medium green amazonite #32 from Pearl, Routt County, Colorado. The spectra are the superposition of the B and G types such that the relative intensity of the 625 and 720 nm bands gives one apparent very broad band. Spectra taken at 77 K resolve the two bands. (d) Blue-green type T amazonite #21 from pegmatites near Keivy, USSR. The most intense absorption for the type T color is shifted to 643 nm and is broader than the singlet of the blue amazonites. Broad bands are also present at 385 nm (shown here) and revealed at 330 nm by irradiation.

Table 1. Sample description and chemistry of amazonite and other feldspars in order of increasing Pb content

Sample Number	Museum Number	Locality	Color Munsell#	Description	Electron Microprobe Analyses Or	Ab	An	PbO	FeO_{total}	Emission Spect.† Pb	Fe	H_2 Manometry¶ Total H_2
1	13757	Elizabeth R Mine, Pala, CA	NR 9.25	White perthite gemmy parts	95.7	4.3	0	ND	BLD	-	-	0.14
7	15063	Elizabeth R Mine, Pala, CA	NR 9.0	White perthite gemmy parts	-	-	-	-	-	0.005	0.001	0.10
25	9370	White Queen Mine, Pala, CA	NR 9.0	White perthite gemmy parts	-	-	-	-	-	-	-	0.13,0.15
8	15067	Wigwam Creek, CO	7.5BG9/2	Pale blue, turbid mottled perthite	(99	1	0)	-	-	0.015*	0.01	-
14	15058	Hawthorne, Nevada	2.5B8/4	Bright blue perthite	-	-	-	-	-	0.020	0.015	-
15	15105	New York Mts, CA	5Y9/2	Grey perthite	(95	5	0)	-	-	0.030	0.030	-
16	15055	Landsverk Norway	7.5BG7/8	Blue turbid perthite	-	-	-	-	-	0.030	0.015	-
4	DMNH-10934	Wigwam Creek, CO	7.5BG7/7	Blue zoned perthite	(97.2	2.5	0)	-	-	0.045*	0.030	-
23	10102	Chittaranjan, Bahir, India	7.5BG7/6	Blue, zoned coarse perthite	94.3	5.6	0.1	0.05	BLD	-	-	-
5	15020	Lake George Colorado	7.5BG6/8	Dk. blue perthite with white overgrowths on selected faces	(95	5	0)	-	-	0.050	0.030	0.06,0.07
12	15020	Lake George Colorado	7.5BG7/8	Blue turbid perthite	95.7 (95	4.3 5	0 0)	ND -	trace -	0.07	0.07	0.09,0.15,0.17
18	15056	Jose Bukuru Paddock, Nigeria	10G7/4	Grey-green opaque microperthite	(97	3	0)	-	-	0.07	0.15	-
22	-	Amelia, VA	10G7/8	Green perthite	94.8	5.2	0	0.085	BLD	0.10*	0.07	-
24		Amelia, VA	NR 9.5	White section from #22	95.2	4.8	0	0.12	BLD3	0.10*	0.03	-
19'	13758	New York Mts, CA	2.5BG7/6	Blue-green turbid perthite	90.7	9.3	0	0.19	0.01	0.07	0.003	-
19	13758	New York Mts, CA	2.5BG7/2	Blue-green turbid perthite	(93	7	0)	-	-	0.20	0.015	-
9	15020	Lake George, Colorado	5BG6/8	Green-blue perthite	93.7 (95	6.3 5	0 0)	0.20	0.05	0.12*	0.02	0.09
21	15021	Keivy, Kola Penn., USSR	2.5BG5/6	Dk. blue-green w/ coarse white albite blebs	95.5 (95	4.5 5	0 0)	0.20	0.03	0.10	0.03	0.11
20	15057	Monapo, Mozambique	7.5BG8/6	Med. green turbid perthite	(92.8	7.1	0	1.0)	-	0.30	0.015	-
32	15065	Pearl, Routt Co., Colorado	5G9/2	Green coarse perthite	94.2	5.7	0.1	0.81	BLD	0.70	0.07	-
6	15066	Keivy, Kola Penn., USSR	7.5G6/8	Malachite green w/ coarse white albite blebs	95.3 (95.5	4.6 4.5	0.1 0	0.83 1.0)	BLD -	1.0*	0.03	-
26	15059	El Rancho, Jefferson Co., Colorado	5G9/2	Grey-green turbid with grey inclusions	93.9	6.1	0	1.10	BLD	0.70§	0.015	-
3	13756	Broken Hill, N.S.W., Australia	2.5G7/2	Grey-green orthoclase with grey inclusions	94.2 (94.4	5.7 5.6	0.1 0	1.79 1.75)	trace -	2.0	0.07	-
3'	13756	Broken Hill N.S.W., Australia	2.5G7/6	Med. green orthoclase	91.3	8.7	0	1.60	BLD	-	-	-
3"	13756	Broken Hill N.S.W., Australia	2.5G6/8	Green orthoclase	92.1	7.6	0.3	1.80	BLD	-	-	0.12

All analyses are in weight%, except that Or, Ab, An are in mole %. Probe values in parentheses are from Foord (Pers. Comm.)
*Emission spectrographic analyses are from (Foord and Martin, 1979) §Not pure,
†All emission spectroscopy data, except for samples with* are from (Foord, Martin, Conklin, and Simmons, in prep)
BLD = below limit of detection. ND = not determined. ¶Multiple values are from duplicate runs.

Table 2. Optical absorption parameters of natural amazonites

Color Type	Sample Number		Visible Peak 1/λ cm-1	$W_{1/2}$ cm-1	I cm-1	II cm-2	UV-Vis Peak 1/λ cm-1	$W_{1/2}$ cm-1	I cm-1	II cm-2	UV Peak 1/λ cm-1	$W_{1/2}$ cm-1	I cm-1	II
B	8	β	16000	>2500	1.13	>2825	~26200	~3000	0.6	~1800			ND¶	
		α	"		~0		"		~0				ND	
B	5	β	16050	3350	8.4	28140	25780	3500	5.5	19250	30770	2700	6.1	16470
		α	16000	"	1.7	5700	"	"	1.1	3850			ND	
B	12	β	16000	3350	10.1	33840	26000	3500	6.6	23100			ND	
		α	"	"	2.2	7370	"	"	1.3	4550			ND	
B	9	β	16000	3450	8.72	30080	25800	3150	5.9	18585	30860	2850	5.9	16815
		α	"	"	1.15	3970	"	"	1.15	3625			ND	
T	21	β	15530	3760	13.16	49480	25700	~4000	8.16	~32600	30824		ND*	
		α	"	"	2.7	10260	"	"	1.32	~5300			ND*	
D	23	β	15700	3760	3.50	13160	26000	3350	~2	~6700	30000	?	~2	~6000?
		α	15880	3400	0.71	2430	"	"	0.4	1340			ND	
D	22	β	14840	4380	4.40	19270	25700	3900	3.52	13730	31100	3000	3.96	~1900
		α	"	"	1.10	4820	"	"	~0.50	~2000	"	"	~0.50	~1500
D	19'	β	14840	~4500	6.84	~30800	~26000	3350	4.21	14100			ND	
		α	"	"	1.68	~7600	"	"	weak				ND	
D	6	β	14840	~4230	12.1	~51180	26000	~3700	~9	~33300			ND	
		α	"	"	2.2	~9300	"	"	~1.6	~5900			ND	
D	32	β	14180	4090	5.26	21510	25600	~3800	4.21	~16000	29000	3050	4.56	13900
		α	"	~3800	1.75	~6660	"	"	1.75	~6650	"	"	1.75	5350
G	26	β	13710	3100	4.20	13020	28500?		v wk†		31300?		v wk	
		α	"	"	0.95	2950			ND				ND	
G	3"	β	13700	3000	11.10	33300			?		29400?		v wk	
		α	"	"	2.94	8820			?		"		"	

1/λ is the peak position, $W_{1/2}$ is the full width at half height, I is intensity, and II is the integrated intensity
* This band is weakly present in gamma, and strongly present in an irradiated sample in beta and moderately in alpha
† Very weak
¶ Not determined

doublet; like the type B spectra, the type T has both 385 and 330 nm bands present.

The parameters of the peak(s) at 625 to 720 nm in beta are sufficient to quantitatively describe amazonite color because: (1) The integrated intensity in the alpha polarization is linearly correlated with that in the beta polarization for each of the 625 to 720 nm peaks and the 385 nm peak (Fig. 2).[3] Sufficient data were not available on the 330 nm peak to establish this correlation. (2) The integrated intensity for each of the 385 and 330 nm peaks is a linear function of that of the band(s) at 625–720 nm (Fig. 3).[3] Table 3 summarizes the optical properties of the 630–720 absorption for all amazonites examined.[3]

Response of color to heating and irradiation

Amazonite color can be removed by heating and regenerated by irradiation only if the heating is applied below about 500°C and for less than about 1/2 hour. Otherwise, color is at best only partially restorable. After extensive heating, the blue or green color cannot be recovered: instead, a smoky color similar to smoky quartz occurs. Without prior heating, amazonite color can increase, decrease, or remain the same after gamma irradiation (Tables 3 and 4);[3] this implies that only color saturated through radiation should be compared to the chemistry.

The kinetics of amazonite coloration were determined by monitoring the intensity of the near-IR peak as a function of γ-ray dose (Table 4). Coloration is initially rapid but saturation occurs at about 100 MRads. The data are best fit by a first order rate law:

$$\frac{dX}{dt} = -k(C - X). \tag{2}$$

where X is the number of color sites present at a given time, and C the maximum number available. Integration from 0 to t and rearranging gives

$$\ln (1 - X/C) = -kt. \tag{3}$$

Representing the number of color sites by the intensity, and estimating C from the saturation color gives the graphical representation of Figure 4; the slopes are sample-specific.

Relationship of amazonite color to lead content

Amazonite becomes greener and usually, but not always, more intensely colored with increasing lead content (E. E. Foord, pers. commun.). The hue changes with increasing Pb because (1) type B spectra occur for amazonites with low lead contents; (2) type G only occurs for samples having greater than 1% Pb, and (3) for type D and T, the average peak energy decreases with increasing Pb, due to

[3] Figures 2 and 3 on amazonite peak parameters, Figure 9 of near-IR spectra of water in feldspar, Table 3 of optical properties, Table 5 of EPR properties, and Table 7 of the dehydration of amazonite may be obtained from the authors or by ordering document AM-85-271 from the Business Office, Mineralogical Society of America, 2000 Florida Ave., N.W., Washington D.C. 20009. Please remit $5.00 in advance for the microfiche.

Table 4. Irradiation response of 625 to 720 nm band of selected amazonites

Sample Number	$W_{1/2}$ cm-1	Dose, MRads	I, cm-1	C, cm-1	1-I/C	k_1, MRads-1
12 heated (450°C)	3300	0	4.1	9.7	0.58	0.0277
		6	4.8		0.51	
		20	6.5		0.33	
		45	8.1		0.165	
		70	8.9		0.082	
		121	9.5		0.021	
3"	3000	0	9.5	14.0	0.321	0.0230
		11	10.1		0.279	
		29	11.2		0.200	
		40	12.4		0.114	
		67	13.1		0.064	
		94	13.4		0.040	
		145	13.85		0.011	
3" heated (300°)	3000	0	3.2	6.5	0.508	0.0230
		18	4.1		0.369	
		29	4.8		0.262	
		56	5.4		0.169	
		83	6.0		0.077	
19'	4500	0	6.7	9.37	0.284	0.0852
		15	8.4		0.103	
		25	9.0		0.0039	
		76	9.36		0.001	
4	3300	0	5.95			
		10	5.75			
		35	4.68			
21	3800	0	13.16			
		25	11.7			
		91	11.2			

I is the intensity measured. C is the estimated maximum intensity obtainable through irradiation. k_1 is the slope of the line defined by ln(1-I/C) as a function of dose of 1.41 Mrads/day.

an increase in the 720 nm peak relative to the 630 nm component with increasing Pb content. The intensity of the color is related to the integrated intensity of bands near 630–720 nm. Figure 5 shows that the integrated intensity generally increases with lead content for the low Pb samples, but there is no common trend for all samples; because the eye is more sensitive to green than to blue, visual assessment suggests a continuous trend.

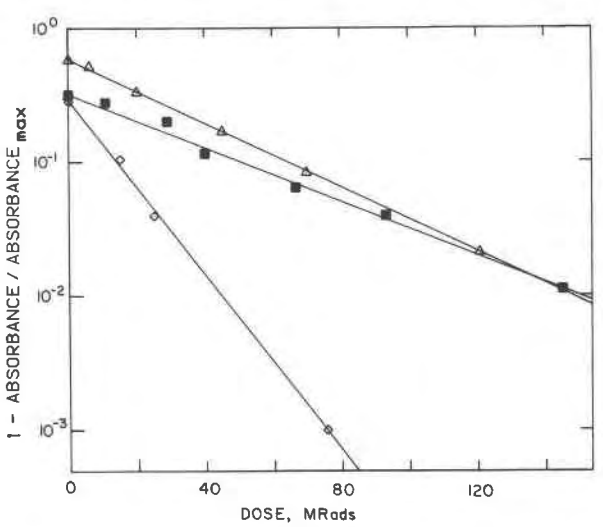

Fig. 4. Logarithmic plot of 1-absorbance/absorbance$_{max}$ as a function of cumulative radiation dose. Triangle = B #12. Diamond = D #19'. Square = G #3". The constants differ for each sample (see Table 4), and the linear correspondence implies first-order kinetics.

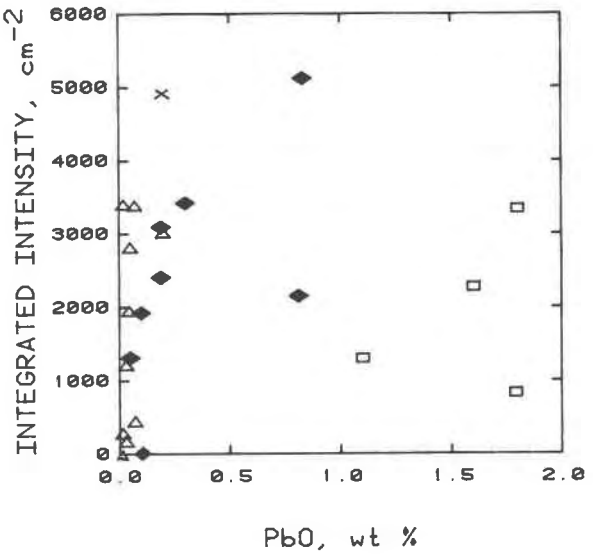

Fig. 5. Dependence of amazonite peak parameters on lead content of natural amazonites. Triangle = type B. Diamond = type D. Square = type G. X = type T. For integrated intensity for low lead contents, intensity generally increases with lead content, but this correlation is statistically insignificant and beyond 0.5 wt% no clear cut trend is visible.

EPR spectroscopy of amazonite color centers

EPR spectra were measured for each of the four different amazonite color types and for samples which had been first heated to remove the amazonite color, and then irradiated to reveal centers extraneous to amazonite coloration. For Broken Hill orthoclase, no signal could be attributed to the green color. For all microclines examined, a distinct set of signals (consisting of a large first derivative near $g_{eff} = 1.56$ with two smaller satellite absorption-emission features at $g_{efff} = 1.83$ and 1.38) was observed in the blue-green samples, but not in the heat-bleached and irradiated samples (Fig. 6a). The presence of two or three of these sets in some samples (Fig. 6b) probably reflects the principal values of the anisotropic g-factor and hyperfine interaction, A (G. Lehmann, pers. commun., 1984). The absence of amazonite-type EPR signals in orthoclase may be attributed to signal broadening resulting from disorder (cf. Fe^{3+} in potassium feldspar: Marfunin et al., 1967; Gaite and Michoulier, 1970) in that broadness in a low intensity signal could easily render it invisible.

The sum of the DII for each of the three EPR regions calculated using equation 1 (Table 5)[3] depends linearly on the sum of the integrated optical intensities in the alpha and beta polarizations (Fig. 7). The slight deviation of the one type D sample may be due either to uncertainty in

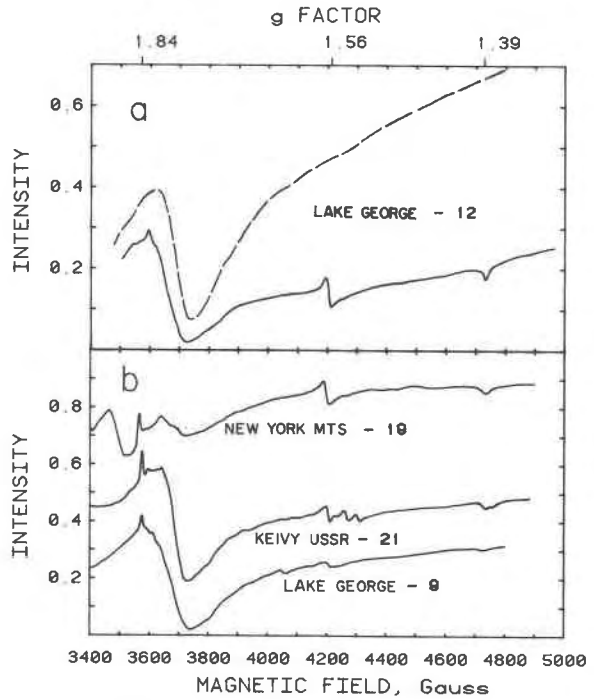

Fig. 6. First-derivative EPR powder spectra taken at 77 K. Spectra are scaled for 100 mg sample weight and run conditions of 1.0 mW, 1G modulation and $\times 1000$ gain. Frequencies were 9.194 GHz except for #19 ($\nu = 9.18$ GHz). The large, broad band near $g_{eff} = 1.8$ is probably due to hematite inclusions. (a) Amazonite #12 from Lake George, Colorado. Solid line, natural blue color (type B). Dashed line, the same sample heated at 900° for 1/2 hour and irradiated (grey). Features near $g_{eff} = 1.83$, 1.56, and 1.39 are connected with amazonite color. (b) Top, #19′, doublet from New York Mountains, 28 MRad dose. Middle, #21, type T, Keivy, USSR, natural. Bottom, #9, blue amazonite from Lake George, Colorado, natural. Smaller features near 3480 and 3640 Gauss are due to the Al-O^- hole center (Hofmeister and Rossman, 1984). All samples have the same features as amazonite #12, but #9 and #21 show additional similar features at slightly different positions, and with much lower intensities.

peak areas or to differences in optical extinction coefficients for the B and G peaks; because the deviation cannot be explained using the intensity of only the 625 nm component, the "color" of all varieties (types B, T, D, and therefore G) arise from the same color centers.

Marfunin and Bershov (1970) reported single crystal g-values of 1.39, 1.56, and 1.837 for an EPR center connected with amazonite color, and attributed this center to Pb^{1+}. These g-values are similar to ours, suggesting that the centers are the same. The following factors support their assignment of the amazonite color center to Pb: The large central first derivative peak with two satellites (Fig. 6a) suggests that the isotopes of the element involved are dominantly of zero nuclear spin, with a small proportion having I = 1/2. The lineshapes of the two satellites are absorption-emission rather than first derivative, probably due to the averaging of anisotropic spectra by the powder method. From Figure 7, the ratio R of the more accurately determined satellite to the central component ranges from 5.5 to 7.1. Theoretically, this ratio is predicted from the isotopic abundances by

$$R = (2I + 1) \cdot \%(I = 0)/\%(I) \quad (4)$$

(Goodman and Raynor, 1970, p. 219). The element whose abundances show the closest correspondence is lead (22.6% I = 1/2, 77.4% I = 0, R = 6.85). For 10^9 year old Pb (appropriate for most amazonites), the model of lead isotopic change by Stacey and Kramers (1975) gives a value of R = 7.1. The only other elements which give comparable ratios are Sn, W, and Pt. Not only is the value of R for Pb closest to the experimental ratio, but Pb is strongly concentrated in amazonites whereas Pt, Sn, and W have not been detected (Foord, pers. commun.). Thus, Pb colors amazonite blue to green; the charge state must be +3 or +1 in order to yield an EPR signal, but powder spectra cannot be used to differentiate between Pb^+ and Pb^{3+}.

The relationship of color to the concentrations of Pb and structural water

Heating above 500°C removes an essential ingredient of amazonite color. Structural changes do not occur at such low temperatures, as indicated by similar IR spectral patterns of vibrations before and after heating (except for the water bands near 3600 cm^{-1}: see below). However, volatile species are likely to be lost over the temperature range in which amazonite color is affected.

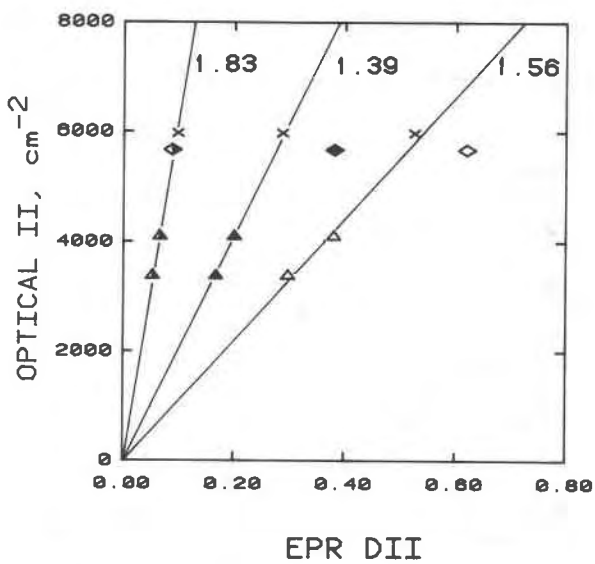

Fig. 7. Dependence of EPR doubly integrated intensities on the sum of the integrated intensity of absorption bands in beta and alpha near 630 to 720 nm. Triangle, type B. Diamond, type D. X, Type T. The lines are labeled with g_{eff} for the three EPR signals. EPR DII scaled for 100 mg same weight, and run conditions of 1 mW, 1G modulation and $\times 1000$ gain.

Speciation of water in amazonite

A typical IR spectrum of microcline-amazonite shows mostly broad bands (Fig. 8a). Cooling the sample with liquid nitrogen splits the broad bands into three components, nearly doubles the intensity, and shifts the central absorption to 3200 cm^{-1}. This indicates formation of ice, showing that the broad, isotropic (with respect to one face) bands are due to fluid inclusions (Aines and Rossman, 1984). Band intensities on spectra taken from the two different faces are not equivalent because a higher density of fluid inclusions occurs perpendicular to (001), as is readily observable through a microscope, producing the difference between α of (010) and α of (001), as seen in Figure 8b. For fluid inclusion water in microcline, an average molar extinction coefficient (ε) of 23 liter/mole·cm ($\pm 5\%$) in α on (010) at 3440 cm^{-1} was determined from IR spectra and total water contents of samples #5, 9, and 12.

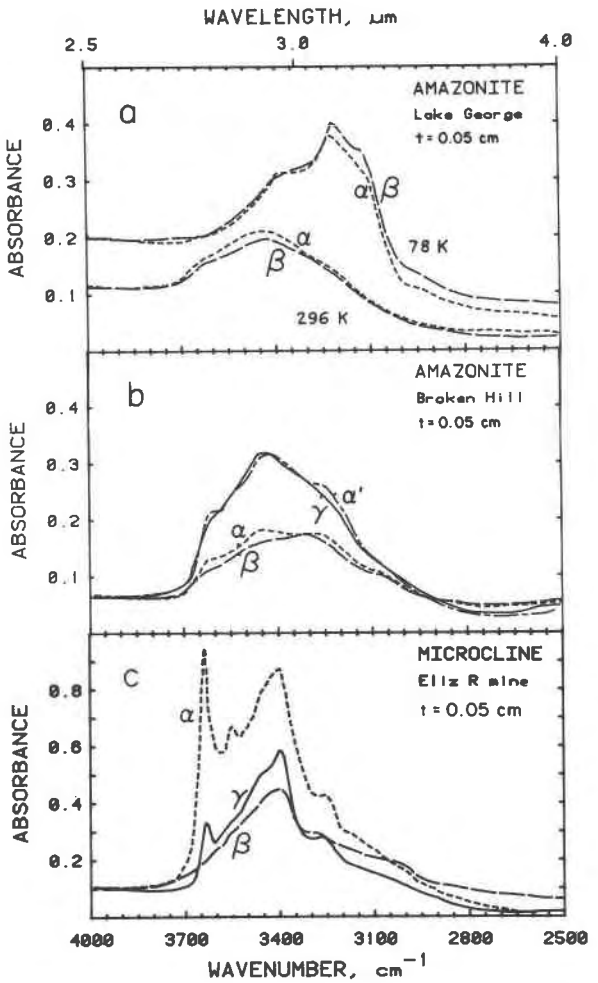

Fig. 8. Polarized infrared spectra of water in feldspar. (a) Amazonite #5 from Lake George, Colorado. The lower pair was taken at room temperature, and the upper pair was taken after the sample was cooled with liquid nitrogen. (b) Green orthoclase #3 from Broken Hill, N.S.W., Australia. Spectral data were scaled from 1 nm and 1.6 mm thick samples. The $\gamma\alpha'$ pair is from (001) while $\alpha\beta$ are from (010). (c) Gemmy area of white microcline #7, Elizabeth R Mine, Pala, CA. Absorption bands present at 3630, 3550, 3460, 3400, 3250, and 3050 cm^{-1} are due to two different types of water molecules.

There is a variable amount of anisotropy in microcline-amazonite IR spectra at 3630 and 3240 cm^{-1}. IR spectra of nearly gem quality green orthoclase from Australia (Fig. 8b) show anisotropy in intensity at four band positions (3630, 3550, 3440 and 3240 cm^{-1}). These positions are the same as those of bands of structural water in white microcline (see below), and show that a small fraction of the water in amazonite may be incorporated in the feldspar structure.

Infrared spectra from the least turbid regions of three white microclines from the Elizabeth R mine and one from the White Queen mine shows two pairs of polarized bands (Fig. 8c). One pair (3630 and 3550 cm^{-1}) is polarized strongly in alpha and weakly in beta. The other pair (3400 and 3250 cm^{-1}) is less strongly polarized. Near-infrared spectra taken on thicker sections of the same crystal (Fig. 9)[3] show two strongly polarized bands of H_2O at 1900 and 1950 nm ($\sim$5250 cm^{-1}), but OH bands are not detected at 2200 nm (4550 cm^{-1}) in agreement with Solomon and Rossman (1979). Correlation of the intensity of the 1900 nm absorptions with that of the fundamentals along with the absence of the 2200 nm X-OH band indicates that hydrogen is present as H_2O in these microclines (Hofmeister, 1984). Because IR spectra taken on white microcline at liquid nitrogen temperatures were not noticeably different from the room temperature spectra, the water indicated by bands at 3630, 3550, 3440, and 3240 cm^{-1} in the IR and 5130 and 5260 cm^{-1} (1950 and 1900 nm) in the near-infrared occurs as isolated molecules in the feldspar structure (structural water). From sample 7 that had the least amount of fluid inclusion water, the molar absorptivity, ε, was calculated as 120 liter mole·cm in α at 3630 cm^{-1}. A possible site for the water is the M site, due to its size; charge balance could occur by substitution of a divalent cation (Pb^{2+}?) for a nearby K^+, or by replacing Al^{3+} with Si^{4+}.

Dependence of color on structural water content

Infrared measurements of the water regions in all amazonites were made (Table 6). Structural water concentrations greater than about 7 ppm are accurate to ± 1 ppm; however, concentrations below 5 ppm are subject to a much larger error due to the difficulty of measuring the height of the 3620 cm^{-1} peak on top of the fluid inclusion band. Uncertainties in the fluid inclusion water contents are $\pm 10\%$, due to inhomogeneity.

The variation in color, fluid inclusion water, and structural water for the 3 samples from Broken Hill (which otherwise had the same chemically) suggests that color depends on structural water and not on fluid inclusion water (Fig. 10).

Pieces of type B sample #12 were heated at various

Table 6. Infrared water absorptivities, derived water content, and infared order parameters of amazonite

Sample Number	I(3620)¶ cm-1	Structural H_2O, ppm	I(3440)§ cm-1	Fluid Inclusion H_2O, ppm	d/m†
7	12.2	1000	~0	~0	1.40
8	~0.2	~12	2.47	820	3.63
14	0.7	42*	5.00	1670	2.72
15	~0.03	~2*	~25	~8000	1.57
16	0.23	14	7.0	2300	3.61
4	0.10	7	2.1	700	4.54
23	0.16	9	1.76	590	3.64
5	0.31	18	2.69	900	1.58
12	0.34	19	4.4	1470	2.88
12 heated	0.196	11	2.82	940	-
18	~0	~0	~56	~18000	0.49
22	0.28	15	2.35	780	2.30
24	~0	~0	4.05	1350	1.30
19	0.20	12	9.1	3000	3.07
19'	0.25-0.42	13-23	5.8	1930	1.69
9	0.15-0.2	8-12	2.76	920	2.94
21	0.13-0.27	7-15	1.60	530	3.10
20	~0.15	~8	~1.7	~560	3.06
32	~0.20	~12	2.53	840	1.18
6	~0.12	~7	1.58	530	3.62
26	0.25	14	4.90	1630	0.83
3	0.31	17	2.5	840	0.21
3'	0.41	22	2.11	700	0.15
3"	0.64	35	2.0	670	0.57

* Molar Pb <molar H_2O
¶ Absorptions due to fluid inclusions and clay subtracted; intensity measured on alpha
§ Absorptions only due to fluid inclusions; intensity taken from α
† This quantity was determined from IR spectra as shown in Figure 13 and was uses as an indication of Al/Si order/disorder

temperatures for 1/2 hour, and then irradiated at a fixed dose. Monitoring the change in water present by infrared spectroscopy showed that heating decreased the concentrations of both fluid inclusion and structurally-bound water at similar rates (Table 7)[3]. The color developed after irradiation is linearly dependent on structural water concentrations for less than 12 ppm H_2O (Fig. 11), with saturation in color occurring above 12 ppm. This shows that most but not all of the structural water present is involved in amazonite color centers.

Evidence for Pb: H_2O = 1:3 in color centers

For the type B and G amazonites in which the molar concentration of Pb exceeds that of structurally bound H_2O, the integrated intensity of the color depends linearly on the concentration of structural water (Fig. 12). Samples 14 and 15 have a lower molar concentration of Pb than of H_2O; these were included in Figure 12 by plotting the molar amount of water equal to their molar amount of lead. That samples #14 and 15 fall on same trend as the other samples strongly suggests that Pb and structural H_2O occur in a one to one ratio in amazonite color centers. The occurence of some doublets outside the trends defined by the type B and type G samples may be related to the partitioning of water among the two different types of color sites. The one type T sample also lies outside the B or G trends, but this is probably due to differences in molar absorptivity for the three different amazonite peaks. Some of the scatter may also be attributed to not all of the structural water being involved in color centers (e.g., #12).

If Pb and H_2O are statistically distributed among the M-sites of amazonite, the probability of H_2O having the closest M site occupied by Pb ranges from 0.06 to 1%. Thus, either H_2O must affect the radiative transformation of Pb^{2+} from afar, or Pb and H_2O occur as a coupled pair in the feldspar. Insofar as irradiation does not change the IR water spectra, then if H_2O affects the irradiative transition regardless of distance to Pb, eventually all ordinary lead would be transformed to the chromophore. This does not happen because under irradiation the intensity of color in orthoclases grows only slightly larger than that of microclines with 1/100 the amount of Pb. Thus, it is likely that much of the structural water is locally coupled with Pb, possibly during growth, by the substitution.

$$Pb^{2+} + H_2O = 2K^{+}. \quad (5)$$

Calculation of extinction coefficients and comparison of amazonite color centers to Pb^{3+}, Tl^{2+}, and Tl° centers in KCl

Extinction coefficients were calculated from the two trends in Figure 12, using effective molar lead contents equal to the molar water concentrations. For type B amazonite, $\varepsilon = 4300$ liter/mole·cm, and for type G, $\varepsilon = 2500$ liter/mole·cm. Oscillator strengths f # calculated from

$$f\# = 4.6 \times 10^{-9}\, \varepsilon\, W_{1/2} \quad (6)$$

are given in Table 8, along with those of Tl^{2+} and Tl° in

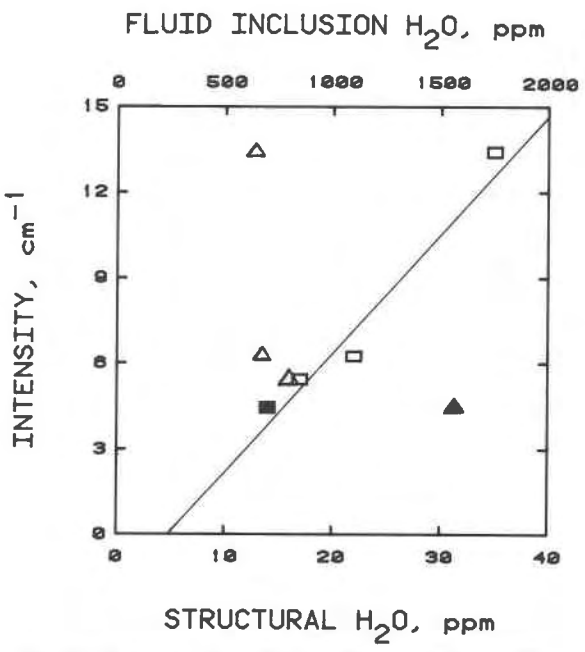

Fig. 10. Variation of radiation-enhanced color with water species in amazonite-orthoclase. Squares (lower axis), structurally bound water. Triangles (upper axis), water occurring as fluid inclusions. Open symbols are samples from Broken Hill #3, 3', and 3"; the filled symbol represents sample #26. Because of the "blank" in the H_2 manometer measurements of a few ppm, the line does not intersect the origin.

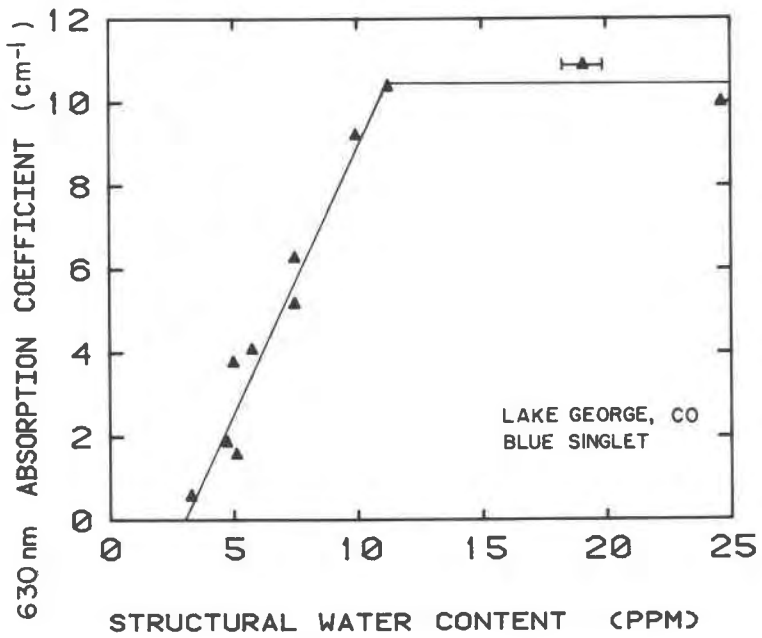

Fig. 11. Variation of intensity of color with structural water by dehydration of amazonite #12, Type B from Lake George, Colorado. Dose, 40 MRads. Saturation occurs above 12 ppm H_2O.

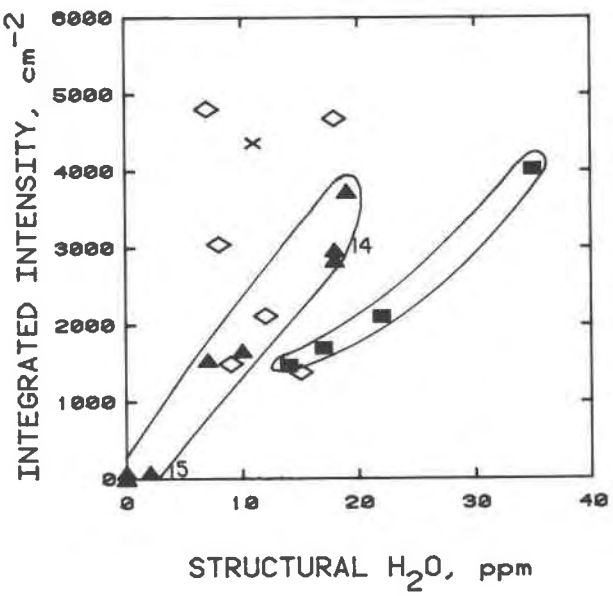

Fig. 12. Dependence of irradiation enhanced amazonite color on structural water content. Filled triangles, type B blue singlets. Open diamonds, type D doublets. Filled squares, type G green singlets. X, type T blue-green singlet. Samples #14 and 15 have higher molar concentrations of water than lead, and were plotted as discussed in the text. The envelopes enclose the two end-member color types. Both a triangle and a diamond (not shown) intersect the origin of both graphs.

KCl which are isoelectronic with Pb^{3+} and Pb^{1+} respectively.

Pb^{3+} produces three bands in KCl at 465, 303, and 216 nm (Schoemaker and Kolopus, 1970), but the oscillator strengths were not measured. The amazonite absorption pattern resembles that of Tl^{2+} in that both have nearly equal strength absorption bands (Table 8). The difference in the number of bands is of unknown significance because amazonite may have a fourth band at the uninvestigated shorter wavelengths. Amazonite spectra resemble those of Tl° in that both have a band at about 625 nm; however, unlike amazonite, the 625 nm band in Tl° is 10 times stronger than the higher energy bands, and additional bands are present at lower energy. This comparison suggests that Pb^{3+} is the chromophore in amazonite rather than Pb^{1+}.

Table 8. Oscillator strengths of amazonite, Tl^{2+}, and T°

Substance	λ, nm	f#	Reference
Amazonite, B	625	0.063	this work
	385	0.042	"
	330	0.036	"
Amazonite, G	720	0.036	"
KCl:Tl2+	364	0.13	Delbecq et al., 1966
	294	0.22	"
	262	0.14	"
	220	0.22	"
KCl:Tl°	1500	8.1 x 10-5	"
	1260	9.3 x 10-5	"
	640	0.48	"
	380	0.03	"
	~340	not determined	"

Relationships between amazonite color type, feldspar structure and Pb content

The degree of Al/Si order can be determined by infrared spectroscopy from the separation of the two overlapping peaks near 768 and 728 cm^{-1} ($\sim$13 μm) (Hafner and Laves, 1957). As a measure of this separation we used the ratio of the depth of the trough to the height of the overlap, d/m (Fig. 13). The maximum degree of Al/Si order seems to decrease with increased incorporation of Pb into the potassium feldspars (Fig. 14), and at very high Pb content ($\sim$1.5%) only orthoclase has been observed. The various color types are restricted to specific Pb contents and structural states: (1) Type B occurs at low Pb contents; (2) Type G is limited to high Pb and high structural states; (3) Doublets (D) have intermediate Pb content and intermediate structural states. This information agrees with analogous X-ray data: Colorado amazonites with less than about 2000 ppm Pb have $\Delta_{131,1\bar{3}1} \sim 1$ (Foord and Martin, 1979); Mongolian amazonite with 1950 ppm Pb has $\Delta = 0.87$ (Pivec et al., 1981); Norwegian amazonites with 3000 ppm Pb have $\Delta = 0.6$ to 0.8 (Tibbals and Olsen, 1977). The trends of Figure 14 may indicate that incorporation of Pb into potassium feldspar locally changes the structure such that large amounts (about 2%) are sufficient to produce an overall orthoclase structure. The occurence of type G and type B peaks together in samples of intermediate structural state shows that M-sites of end-member microcline and orthoclase geometries exist for Pb.

For intermediate Pb content and low structural state, unusual amazonite coloration occurs, such as for the Keivy #21 sample with three EPR Pb signals. The change in the EPR spectra is accompanied by a 400 cm^{-1} shift in the energy of the optical bands, suggesting an intermediate structure for the chromophore sites in this sample. Possibly, incorporation of a moderate amount of Pb can cause slight distortions from maximum microcline structure.

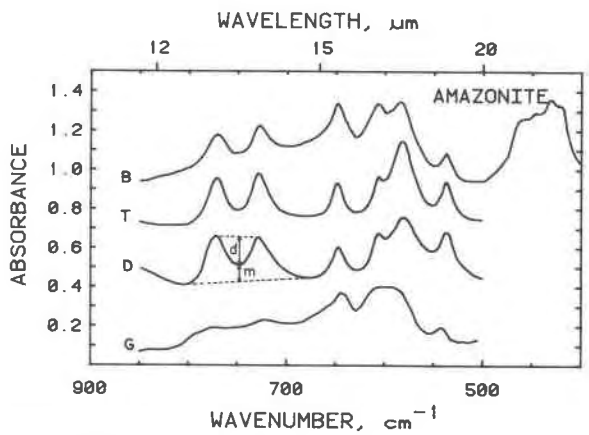

Fig. 13. Infrared powder absoption spectra of amazonites. B, #4 from Wigwam Creek, CO., T, #21 from Keivy, USSR. D, #19′ from New York Mts., CA., G, #3″ from Broken Hill, Australia. Spectra were offset for clarity. The ratio d/m, where d and m are the intensities indicated near 13 μm, was used as a measure of Al/Si order/disorder.

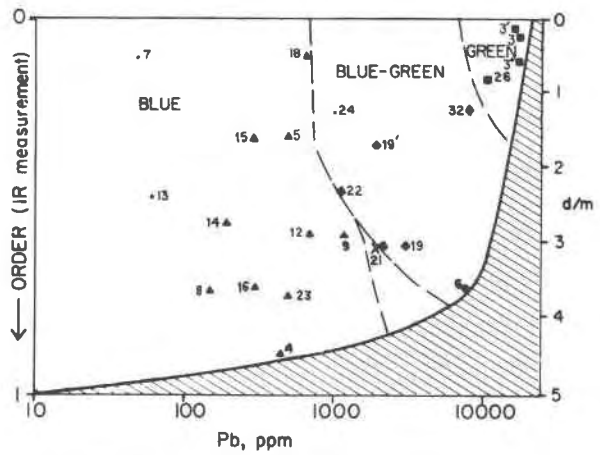

Fig. 14. Order parameter d/m as a function of lead content of amazonites. Dots, uncolored. Triangles, type B. Diamond, type D. Square, type G. X, type T. Dashed lines also show the boundaries of amazonite types.

A model for the mechanism of amazonite coloration

We have shown that (1) amazonite color results from electronic transitions involving Pb^{3+} or Pb^{1+}; (2) the production of the unusual charge state upon irradiation requires the association of a water molecule with the precursor Pb site; (3) irradiative production of color is rate limited by one first order reaction; (4) the speciation and concentration of molecular water are unchanged by the process; (5) different color types are determined by the proportion of the Pb ions located in M-sites with either microcline or orthoclase geometry.

Comparison of the optical spectra of amazonite to those of Tl^{2+} and Tl° in KCl suggests Pb^{3+} as the chromophore in amazonite. Also, Pb^{3+} has been demonstrated to form by irradiation of natural calcite and other oxides (Rohrig and Schneider, 1969; Born et al., 1971; Andlauer et al., 1973; Popescu and Grecu, 1975). Conversely, previous analysis of the EPR center in amazonite suggested Pb^{1+} (Marfunin and Berhov, 1970), as does the g-value of 1.53 for the even Pb isotopes (G. Lehmann and J. Weil, pers. comm., 1984). Perhaps single crystal EPR spectra on several different color types of amazonite would resolve this difficulty.

Points (2) and (4) above suggest that water plays a catalytic role in amazonite coloration. We propose that gamma radiation dissociates water molecules, forming H° ad OH°, radicals that are the primary products of water radiolysis (Draganic and Draganic, 1971). H° has been observed in irradiated hydrous glasses and quartz (Van Wierengen and Kats, 1957; Weeks and Abraham, 1964; Perlson and Weil, 1974). The radical H° probably diffuses and removes smoky color by reduction, as occurs in quartz (e.g. Kats,

1962, p. 194). We suggest that as in quartz (ibid.), hydrogen returns to a site similar to its original one. The radical OH° probably remains stationary, oxidizing nearby oxygens to form hole centers. With both reduction and oxidation occuring, it is possible to form either Pb^{3+} or Pb^{1+}. Natural radioactivity in amazonites (primarily from ^{40}K) is sufficient to produce this color over geologic time (Hofmeister, 1984).

Acknowledgments

Special thanks are due to E. E. Foord (U.S.G.S., Denver) for generously sharing his samples and research ideas with us. Samples were also donated by S. Booth (Zinc Corp. Ltd., Broken Hill, Australia), G. Brown (Stanford), R. Cubba and S. Rigden (Caltech), R. Currier (Jewel Tunnel Imports, Arcadia, California), S. Ghose and A. Irving (U. of Washington), and R. Reynolds (San Bernardino County Museum, California). We thank S. Chan, C. Martin, and D. Blair (Caltech Chemistry Division) for assistance and advice with EPR spectroscopy. Thanks are due to J. R. O'Neil and R. E. Criss (U.S.G.S., Menlo Park) for assistance with hydrogen manometry there. Discussions with L. T. Silver (Caltech) were very helpful. Critical review by E. E. Foord (U.S.G.S., Denver), S. Ghose (U. Washington), G. Lehmann (Muenster), R. F. Martin (McGill U.), and J. Weil (U. Saskatchewan) substantially improved the manuscript. This work was supported in part by NSF grants EAR-79-19987, 79-04801, and 83-13098.

References

Aines, R. D., and Rossman, G. R. (1984) Water in minerals? A peak in the infrared. Journal of Geophysical Research, 89, 4059–4071.

Andlauer, B., Schneider, J. and Tolksdorf, W. (1973) ESR analysis of Pb^{+3} ions in $Y_3Ga_5O_{12}$. Physical Review B, 8, 1–5.

Born, G., Hofstaetter, A., and Scharmann, A. (1971) $2S_{1/2}$-states of Pb^{+3}-ions: correlations between g-values and hyperfine splitting constants A in the EPR Spectra. Zeitschrift für Physik, 248, 7–12.

Cech, F., Misar, Z., and Povondra, P. (1971) A green lead-containing orthoclase. Tschermaks Mineralogische und Petrographische Mitteilungen, 15, 213–231.

Delbecq, C. J., Ghosh, A. K., and Yuster, P. K. (1966) Trapping and annihilation of electrons and positive holes in KCl–TlCl. Physical Review, 151, 599–609.

Draganic, I. G., and Draganic, Z. D. (1971) The Radiation Chemistry of Water. Academic Press, New York.

Eaton, S. S., and Eaton, G. R. (1979) Signal area measurements in EPR. Bulletin of Magnetic Resonance, 1, 130–138.

Foord, E. E., and Martin, R. F. (1979) Amazonite from the Pikes Peak Batholith. Mineralogical Record, 10, 373–382.

Friedman, I. (1953) Deuterium content of natural waters and other substances. Geochimica et Cosmochimica Acta, 4, 89–103.

Gaite, J.-M., and Michoulier, J. (1970) Application de la resonance paramagnetique electronique de l'ion Fe^{3+} a l'edtude de la structure des feldspaths. Bulletin de la Société Francaise de Minéralogie et de Cristallographie, 93, 341–356.

Goodman, B. A. and Raynor, J. B. (1970) Electron spin resonance of transition metal complexes. Advances in Inorganic Chemistry and Radiochemistry, 13, 135–363.

Hafner, St. and Laves, F. (1957) Ordnung/Unordnung und Ultrarotabsorption II. Variation der Lage und Intensitat einiger Absorptionen von Feldspaten. Zur Structur von Orthoklas und Adular, Zeitschrift für Kristallographie, 109, 204–225.

Hofmeister, A. M. (1984) A Spectroscopic Study of Feldspars Colored by Irradiation and Impurities, Including Water. Ph.D. Thesis, California Institute of Technology, Pasadena, California.

Hofmeister, A. M. and Rossman, G. R. (1985) A model for the irradiative coloring of smoky feldspar and the inhibiting influence of water. Physics and Chemistry of Minerals, in press.

Kats, A. (1962) Hydrogen in alpha-quartz. Philips Research Reports, 17, 133–195, 201–279.

Marfunin, A. S., Bershov, L. V., Meilman, M. L., and Michoulier, J. (1967) Paramagnetic resonance of Fe^{3+} in some feldspars. Schweizerische Mineralogische und Petrographische Mitteilungen, 47, 13–20.

Marfunin, A. S. and Bershov, L. V. (1970) Paramagnetic centers in feldspar and their possible crystallochemical and petrological significance. Doklady Akademii Nauk SSSR, 193, 412–414 (transl. Doklady Akademi Nauk Translations, 193, 129–130).

Perlson, B. D., and Weil, J. A. (1974) Atomic hydrogen in α-Quartz. Journal of Magnetic Resonance, 15, 594–595.

Pivec, E., Sevcik, J. and Ulrych, J. (1981) Amazonite from the alkali granite of the Avdor Massif, Mongolia. Tschermaks Mineralogische und Petrographische Mitteilungen, 28, 277–283.

Plyusnin, G. S. (1969) On the coloration of amazonite. (in Russian) Zapiski Vsesoyuznogo Mineralogischeskogo Obshchestva, 98, 3–17.

Popescu, F. F., and Grecu, V. V. (1975) Temperature dependence of Pb^{+3} EPR spectrum. Physica Status Solidi (b), 68, 595–601.

Przibram, K. (1956) Irradiation Colors and Luminescence, Pergamon Press, London, England.

Rohrig, R. and Schneider, J. (1969) ESR of Pb^{3+} in ThO_2. Physics Letters, 30A, 371–372.

Schoemaker, D., and Kolopus, J. L. (1970) Pb^{++} as a hole trap in KCl: ESR and optical absorption of Pb^{+++}. Solid State Communications, 8, 435–439.

Solomon, G. C., and Rossman, G. R. (1979), The role of water in structural states of K-feldspar as studied by infrared spectroscopy. Geological Society of America Abstracts with Programs, 11, 521.

Speit, B., and Lehmann, G. (1982) Radiation defects in feldspars. Physics and Chemistry of Minerals, 8, 77–82.

Stacey, J. S., and Kramers, J. D. (1975) Approximation of terrestrial lead isotope evolution by a two stage model Earth and Planetary Science Letters, 26, 207–221.

Tarashchan, A. N., Serebrennikov, A. I., and Platonov, A. N. (1973) Peculiarities of the lead ion's luminescence in amazonite. Konstitutsiya i Svoistva Mineralov, 7, 106–111.

Tibbals, J. E., and Olsen, A. (1977) An electron microscope study of some twinning and exsolution textures in microcline amazonites. Physics and Chemistry of Minerals, 1, 313–324.

Van Wieringen, J. S., and Kats, A. (1957) Paramagnetic resonance and optical investigation of silicate glasses and fused silica, coloured by X-rays. Philips Research Reports, 12, 432–454.

Weeks, R. A., and Abraham M. (1964) Electron spin resonance of irradiated quartz: atomic hydrogen. Journal of Chemical Physics, 42, 68–72.

Manuscript received, April 12, 1984;
accepted for publication, March 14, 1985.